Structures of ^{201}Po and ^{205}Rn from EC/β^+-decay studies

A. Y. Deo,[1,*] Zs. Podolyák,[1] P. M. Walker,[1] A. Algora,[2,3] B. Rubio,[2] J. Agramunt,[2] L. M. Fraile,[4] N. Al-Dahan,[1,5] N. Alkhomashi,[1,6] J. A. Briz,[7] E. Estevez,[2] G. Farrelly,[1] W. Gelletly,[1] A. Herlert,[8] U. Köster,[9] A. Maira,[7] and S. Singla[10]
[1]*Department of Physics, University of Surrey, Guildford GU2 7XH, United Kingdom*
[2]*IFIC, CSIC - Universidad de Valencia, E-46071, Spain*
[3]*Institute of Nuclear Research of the Hungarian Academy of Sciences, Debrecen, H-4001, Hungary*
[4]*Grupo de Física Nuclear, Facultad CC. Físicas, Universidad Complutense, E-28040 Madrid, Spain*
[5]*Department of Physics, University of Kerbala, Kerbala, Iraq*
[6]*KACST, P.O. Box 6086, Riyadh 11442, Saudi Arabia*
[7]*Instituto de Estructura de la Materia, CSIC, E-28006 Madrid, Spain*
[8]*ISOLDE, PH Department, CERN, CH-1211 Geneva, Switzerland*
[9]*Institut Laue Langevin, 6 rue Jules Horowitz, F-38042 Grenoble Cedex 9, France*
[10]*Indian Institute of Technology Delhi, Hauz Khas, New Delhi-110 016, India*
(Received 9 December 2009; published 24 February 2010)

Several low-lying excited states in $^{205}_{86}$Rn$_{119}$ and $^{201}_{84}$Po$_{117}$ were identified for the first time following EC/β^+ decay of ^{205}Fr and ^{201}At, respectively, using γ-ray and conversion electron spectroscopy at the CERN isotope separator on-line (ISOLDE) facility. The EC/β^+ branch from ^{205}Fr was measured to be 1.5(2)%. The excited states of the daughter nuclei are understood in terms of the odd nucleon coupling to the neighboring even-even core. The neutron single-particle energies of the $p_{3/2}$ orbital relative to the $f_{5/2}$ ground state in ^{205}Rn, and the $f_{5/2}$ orbital relative to the $p_{3/2}$ ground state in ^{201}Po, were determined to be 31.4(2) and 5.7(3) keV, respectively. We tentatively identify a $\frac{13}{2}^+$ isomeric level at 657.1(5) keV in ^{205}Rn. The systematic behavior of the $\frac{13}{2}^+$ and $\frac{3}{2}^-$ levels is also discussed.

DOI: 10.1103/PhysRevC.81.024322 PACS number(s): 21.10.−k, 23.40.−s, 27.80.+w, 29.38.−c

I. INTRODUCTION

One major goal in nuclear structure studies is to understand the interplay between collective and single-particle states and the evolution of deformation away from closed shells. However, information on single-particle structures in the near-spherical $Z > 82$ and $N < 126$ region [1–4] is incomplete. We attempt to bridge this gap by investigating EC/β^+ decays of $^{201}_{85}$At$_{116}$ and $^{205}_{87}$Fr$_{118}$ at the CERN isotope separator on-line (ISOLDE) facility. The study of odd-A isotopes in this region is also of particular interest as the high-j $i_{13/2}$ orbital is in the vicinity of the Fermi surface where the odd nucleon generally occupies comparatively low-j (e.g., $\pi f_{7/2}$, $\nu p_{3/2}$, $\nu f_{5/2}$) orbitals. This gives rise to $\frac{13}{2}^+$ isomeric states in some odd-A isotopes in this region. The excitation energy of this isomer is important in understanding the behavior of both proton and neutron, $i_{13/2}$ orbitals as one moves away from the doubly magic $^{208}_{82}$Pb$_{126}$ nucleus. The present study also aims to shed some light on this topic.

II. EXPERIMENTAL SETUP

In the experiment, a 1.4 GeV proton beam from the CERN PS-booster impinged on a 46 g/cm^2 UC$_2$-C target. On average, every 5.6 s, a pulse of 3×10^{13} protons hit the ISOLDE target. The spallation products diffused out of the 2040°C hot target to a 2120°C hot tungsten tube where francium was surface ionized, accelerated to 30 keV and mass separated by the ISOLDE General Purpose Separator (GPS) set to transport the $A = 205$ products. The surface ionization potential of isobaric elements is significantly higher than for francium, resulting in orders of magnitude lower surface ionization efficiency and, hence, a quite pure beam of francium [5]. These products were collected on a magnetic tape and transported to a measurement station at regular time intervals of 16.8 s. At the measurement station, the source could be viewed by an electron spectrometer and two high-purity germanium (HPGe) detectors.

The electron detection system incorporated a MINI-ORANGE spectrometer [6,7] and a 4 mm thick Si(Li) detector with an active area of 300 mm^2 and resolution of 2.0 keV at ∼500 keV. The detector was cooled to liquid nitrogen temperature with the help of a copper cold finger. For the MINI-ORANGE spectrometer, a set of six equally spaced permanent magnets was used. The distance between the MINI-ORANGE spectrometer and the detector was chosen to be 110 mm so as to maximize electron transmission efficiency in the energy range of 400–800 keV. A central tungsten absorber was used to shield the Si(Li) detector from direct x rays and γ rays. The transmission efficiency curve of the MINI-ORANGE spectrometer was obtained using transitions of well-established internal conversion coefficients from sources of ^{190,194}Hg and ^{203}Pb delivered at different mass settings of the GPS and transitions from the ^{207}Bi source.

The two HPGe detectors were located at 90° and 180° with respect to the Si(Li) detector and the beam direction. They had absolute efficiencies between ∼4% and ∼0.3% and a resolution of 1.0 and 2.0 keV at ∼100 keV and ∼1.5 MeV, respectively. The energy and efficiency calibrations for the

*A.Deo@surrey.ac.uk

HPGe detectors were carried out using ^{133}Ba and ^{152}Eu sources.

The data were collected using a commercially available triggerless digital data acquisition system Pixie4 [8]. In total, five parameters (one signal from the magnetic tape movement, two from the HPGe preamplifiers, one from the Si(Li) preamplifier, and one from the proton pulse) were recorded and time-stamped. The data were sorted offline into four 4k×4k different types of coincidence matrices [γ-γ, γ-conversion electron (CE), γ-time, and CE-time] for further investigations using the RADWARE analysis package [9].

III. EXPERIMENTAL RESULTS

Singles γ-ray spectra showed the presence of several new γ-ray transitions. Figure 1(a) shows part of a singles γ-ray spectrum as recorded in one HPGe detector (with a smooth background subtracted, ~40 000 counts at 600 keV). These β-delayed γ rays were identified in Z from coincident x rays and CE spectroscopy. The conversion electrons corresponding to γ rays in Fig. 1(a) are shown in Fig. 1(b). The following procedure was adopted for the analysis of the data:

(i) Singles γ-ray spectra were searched for new transitions.
(ii) For the new transitions, CE spectra were carefully analyzed. This allows element identification from the difference in γ-ray and CE energies, as well as conversion coefficients.
(iii) The spectra with gates set on these new γ rays were obtained from γ-γ matrices. The x rays in these spectra give confirmation of the elements to which the gated γ rays belonged. This method is particularly helpful in the present work, because *electron capture* is dominant over β^+ decay.
(iv) When possible, γ-CE matrices were also used to strengthen the identification of the new transitions. It was done by setting a gate on a CE transition and looking at the low-energy part of the γ-ray spectrum, which shows the characteristic x rays of the element in which the transition was converted.
(v) Furthermore, γ-time matrices were used to obtain information on the half-life of the parent nucleus populating excited states in the daughter nucleus, which then deexcite by emitting γ rays. Specific values could be obtained only when the half-life was smaller than or comparable to the measurement time at the tape station, which was 16.8 s.

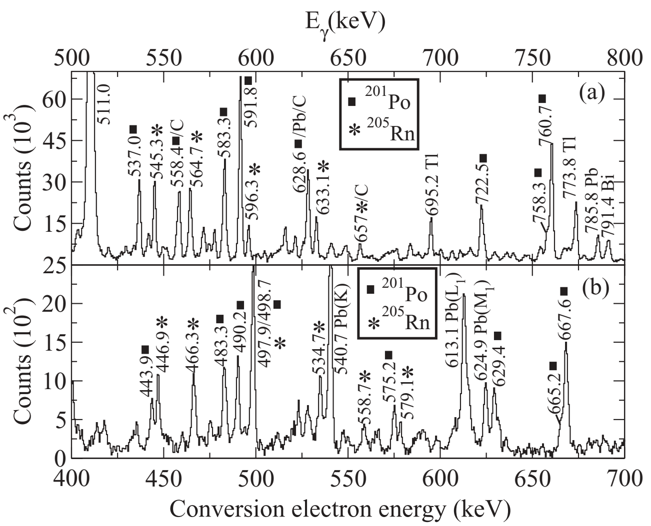

FIG. 1. (a) Singles γ ray and (b) conversion electron spectra. γ rays and conversion electrons are labeled with their energies and the daughter nucleus to which they belong. Tl, Pb, Bi, and the "C" denote γ rays in ^{197}Tl, ^{201}Pb, ^{201}Bi, and long-lived contaminants from a previous experiment, respectively. The energy scales are shifted so that radon γ rays and K-conversion electrons are approximately aligned. K-shell binding energies for Rn and Po are 98.4 and 93.1 keV, respectively. A smooth background generated by RADWARE has been subtracted from the spectra.

The conversion coefficients were obtained from the γ-ray and conversion-electron intensities using the transmission efficiency curve for the MINI-ORANGE spectrometer.

The log ft values were obtained from the intensity balances of the transitions which have been placed in the level scheme assuming no significant β-decay branching to the ground and first-excited states.

The transitions which show only characteristic x rays in coincidence are assumed to directly populate either a ground state, the first excited state (at low energy), or an isomeric state. In the following, we discuss the results obtained using the above procedure.

A. ^{205}Rn

$^{205}_{87}$Fr$_{118}$ decays predominantly by α emission. The ground state $I^\pi = (\frac{9}{2}^-)$ is based on the systematic observation of $9/2^-$ ground states in heavier francium isotopes [10]. An upper limit of only 1% for the EC/β^+ decay to ^{205}Rn was established earlier [10]. Borchers *et al.* [11] have measured the ground state $I^\pi = \frac{5}{2}^-$ for ^{205}Rn using hyperfine interactions and isotope shift techniques. Many positive-parity high-spin states in ^{205}Rn were known prior to this study [12]. Apart from this, only two states at 387.0(5) and 633.7(11) keV were identified by Heßberger *et al.* [4] in the α decay of ^{209}Ra. It was, however, possible to identify a few γ-ray transitions following the EC/β^+ decay in the current study. Some of these γ rays along with their corresponding K-shell conversion electrons are shown in Fig. 1. Furthermore, the different coincidence matrices mentioned in the previous section help confirm the assignment of the transitions to ^{205}Rn. Figure 2 shows the low-energy part of spectra with gates on 633.1 and 564.7 keV γ rays and corresponding K-shell conversion electrons, obtained from γ-γ and γ-electron coincidence matrices. The K_α and K_β x rays clearly confirm their assignment to Rn.

The similarity of the half-lives of the transitions in the daughter nucleus with the parent ground-state half-life further strengthens the evidence of their origin from parent ground-state decay. The γ-time matrix was used to obtain apparent half-lives (see Table I) of some of the transitions. The 503.8 keV transition has a relatively high value for the apparent half-life due to the presence of the poorly resolved 511 keV

TABLE I. γ-ray energies and relative intensities along with the experimental and theoretical [13] K-shell conversion coefficient and assigned multipolarity, for transitions in ^{205}Rn. The uncertainties in the energies are within 0.2 keV.

Transition energy (keV)	Relative intensity (I_γ)	Apparent half-life (s)	Experimental K-conversion coefficient (10^{-2})	Theoretical K-conversion coefficient			Assigned multipolarity
				$E1$ (10^{-2})	$E2$ (10^{-2})	$M1$ (10^{-2})	
356.3	52(4)	4.01(11)	4.8(11)	1.84	4.76	30.24	$E2$
387.5	36(3)		20.5(40)	1.58	4.08	26.17	$M1$
503.8	33(3)	4.60(35)	2.2(5)	0.88	2.33	11.93	$E2$
545.3	98(8)	4.07(5)	1.6(7)	0.76	1.99	9.66	$E2$
564.7	100	3.88(33)	2.2(3)	0.71	1.86	8.81	$E2$
596.3	41(4)	3.86(8)	6.9(9)	0.64	1.67	7.63	$M1$
633.1	63(5)	3.76(11)	2.7(3)	0.57	1.48	6.52	$E2+M1$
657.1[a]							

[a]This transition is highly contaminated. Therefore, it was not possible to extract the experimental parameters. The energy is from conversion electron energy plus K-shell binding energy.

positron annihilation peak. It was not possible to obtain the apparent half-life for the 387.5 keV transition due to a strong contaminant transition from ^{197}Pb. A representative fit to the 545.3 keV γ ray is shown in Fig. 3. The average apparent half-life deduced from all the values quoted in the Table I is 4.03(8) s. This is in satisfactory agreement with the accepted half-life [3.92(4) s] of ^{205}Fr [10]. The resulting level scheme of ^{205}Rn obtained from the above analysis is shown in Fig. 4. The measured K-shell conversion coefficients along with the theoretical [13] values for various transition multipolarities are quoted in Table I. All the transitions to levels in ^{205}Rn have $\log ft$ limits very close to 7 (see Fig. 4) indicating that the levels are populated in the allowed and first forbidden β decays.

Below, we discuss each level in detail:

The 31.4 keV level was established from the energy difference between two pairs of transitions, originating from the levels at 387.5 and 596.3 keV. The spin-parity ($\frac{3}{2}^-$) has been assigned with the help of systematic information from neighboring nuclei (see Fig. 8).

The 387.5 and 596.3 keV levels were both established on the basis of similar arguments. The energy difference between 356.3 and 387.5 keV transitions is consistent with that between 564.7 and 596.3 keV transitions. Also, the fact that no other γ-ray transitions were found in coincidence with these transitions indicates that one of them should populate the ground state. $E2$ multipolarities of 356.3 and 564.7 keV transitions and $M1$ multipolarities of 387.5 and 596.3 keV transitions were obtained from the conversion coefficients (see Table I) further strengthening their placements

The 545.3 keV level was tentatively established via a 545.3 keV $E2$ transition populating the ground state directly. However, the possibility of it populating the level at 31.4 keV cannot be excluded, hence the tentative placement.

The 633.1 keV level was established in the earlier work as 633.7(11) keV [4]. However, no spin-parity assignment was made. The experimental conversion coefficient (see Table I) suggests a mixed, $E2+M1$, nature for the 633.1 keV transition.

The 657.1 keV level was tentatively identified as the neutron $i_{13/2}$ level from the 558.7 keV K-shell conversion electron

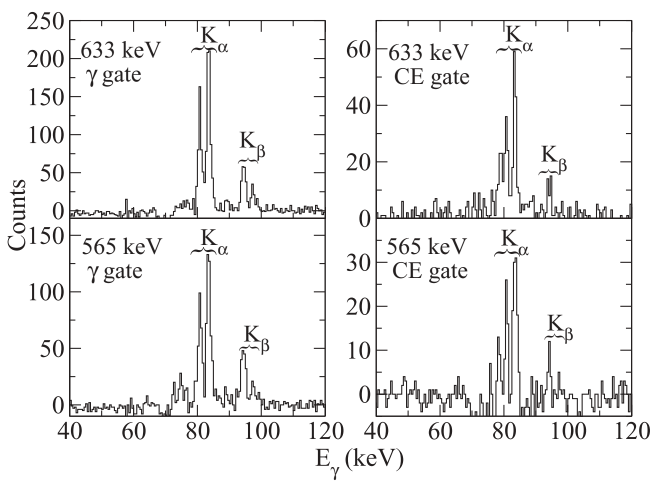

FIG. 2. X-ray spectra obtained from the gates on γ-γ and γ-CE matrices showing K_α and K_β x rays of Rn. The spectra are labeled with corresponding gating transitions.

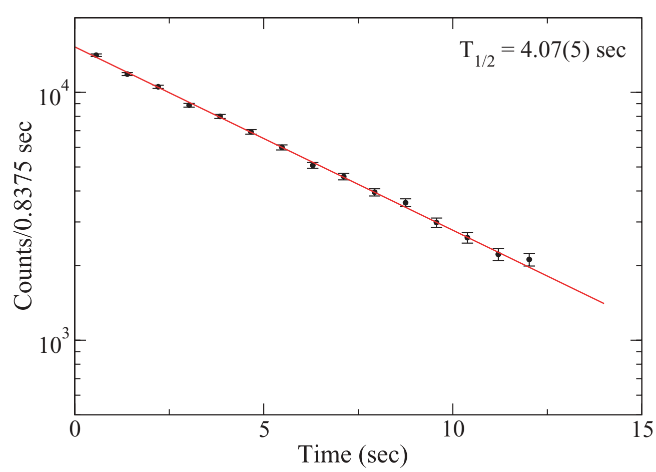

FIG. 3. (Color online) Fit to the decay of a level that deexcites via a 545.3 keV γ ray in ^{205}Rn, which is populated in the EC/β^+ decay of ^{205}Fr.

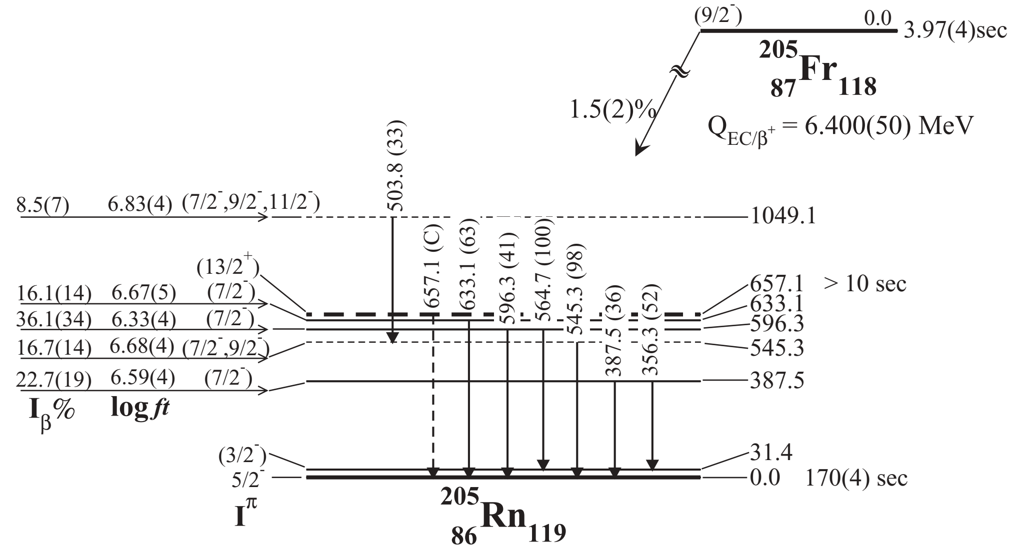

FIG. 4. Level scheme of ^{205}Rn as obtained from the present work. All the transitions are labeled with their energies and relative γ-ray intensities in brackets. Also, all the levels are labeled with their corresponding excitation energies (on the right). "C" indicates that the γ-ray transition is highly contaminated (and for the 657.1 keV transition the placement is based on K-shell conversion electrons). The ground-state half-life of ^{205}Fr is a combination of accepted half-life [10] and that from the present work. The ^{205}Rn ground-state half-life is from Ref. [10], while the Q value is from Ref. [14].

line and needs some explanation. The gate on the conversion electron peak at 558.7 keV in γ-CE matrices shows Rn x rays (see Fig. 5), indicating that the 657.1 keV transition belongs to ^{205}Rn. It was not possible to unambiguously determine its half-life and conversion coefficient, because the 657.1 keV γ-ray was highly contaminated by transitions from very long-lived isotopes (^{76}Br and ^{76}As) from a previous experiment. Nevertheless, from the persistence of CE events over the 16.8 s measurement time, a conservative estimate of $T_{1/2} > 10$ s can be determined. Such a long half-life implies a

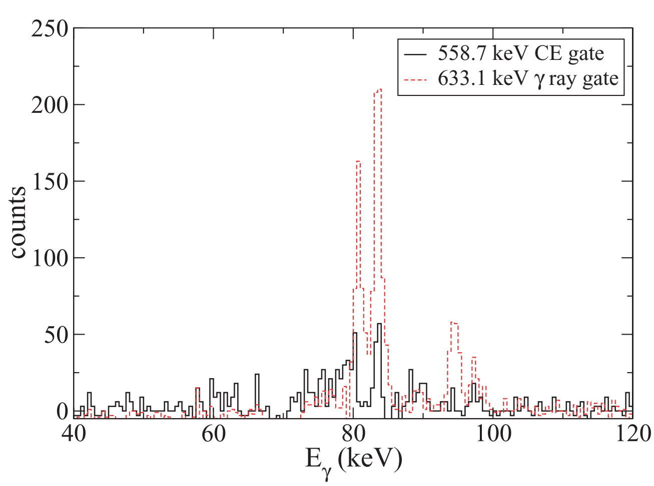

FIG. 5. (Color online) Spectra obtained from gate on the 558.7 keV conversion electron from γ-CE matrices (black curve) and the 633.1 keV γ ray gate from γ-γ matrices (dashed curve), showing K_α and K_β x rays of Rn. The black curve is scaled up by a factor of 3 for ease of comparison.

high multipolarity transition, hence the tentative $i_{13/2}$ neutron level assignment.

The 1049.1 keV level was also tentatively established due to the strong coincidences between the 545.3 and 503.8 keV transitions. From intensity arguments, the 503.8 keV transition is placed above the 545.3 keV transition. It should be noted that the levels at 545.3 and 1049.1 keV are tentative only, because experimental information was not sufficient to determine whether the 545.3 keV transition decays to ground state or the first excited state. If it decays to the first excited state, then the excitation energy of these levels would be 31.4 keV higher than their present values.

The EC/β^+ branching from ^{205}Fr was measured to be 1.5(2)% with the help of γ-ray intensities in ^{201}Po and ^{205}Rn assuming no direct EC/β^+ feeding to the ground and first excited states in these nuclei, and assuming a 29% EC/β^+ decay branch [15] from ^{201}At.

B. ^{201}Po

A large fraction (98.5%) of ^{205}Fr α-decays into ^{201}At, which in turn EC/β^+-decays into ^{201}Po with a half-life of 1.42 ± 0.03 min [15]. However, states in ^{201}Po arising from the EC/β^+ decay of ^{201}At were not known prior to this study. The ground-state spin-parity ($\frac{3}{2}^-$) was established by Axensten *et al.* [16] using atomic beam techniques. Two more negative-parity states were also known at 6.3(23) and 142(3) keV [2]. An 8.9 min $\frac{13}{2}^+$ isomer was known at 423.6 keV from various studies [15]. Apart from this, several high-spin states were known from heavy-ion fusion-evaporation reactions [17]. In our study, it was possible to identify several γ-ray transitions following EC/β^+ decay of ^{201}At for the first time, using the same procedure as that used

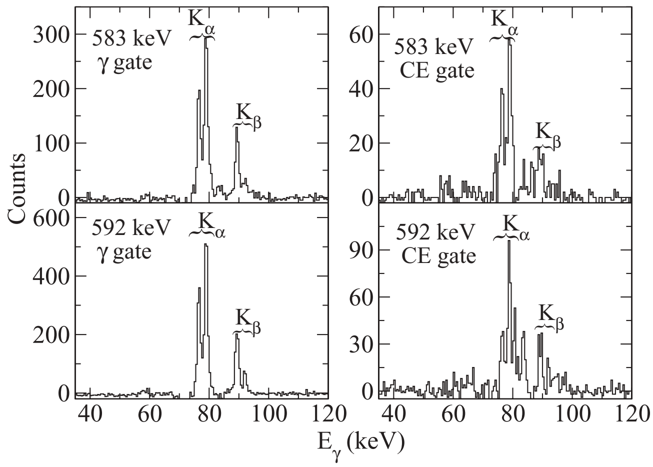

FIG. 6. Spectra obtained from the gates on γ-γ and γ-CE matrices showing K_α and K_β x rays of Po. The spectra are labeled with corresponding gating transitions.

for ^{205}Rn and outlined in the previous section. However, it was not possible to determine the parent half-life in the current work, because it is much longer than the tape cycle time. Some of the new transitions belonging to ^{201}Po are shown in Fig. 1, while Fig. 6 further demonstrates identification of the origin of selected transitions. The deduced level scheme is shown in Fig. 7. All the levels except the ground state, first excited state, and isomeric state have been established in the present work.

The placement of newly observed transitions in ^{201}Po is more complex than in the previous case of ^{205}Rn, due to the presence of the well-known 8.9 min, $\frac{13}{2}^+$ isomer at 423.6 keV. The placements of some of the important levels are discussed below.

The 5.7, 621.6, and 722.5 keV levels: The level at 5.7 keV is fixed from the difference between the 621.6 and 616.1 keV and the 722.5 and 716.6 keV transitions, while the 621.6 and 722.5 keV levels are established from the presence of respective γ-ray transitions.

The 758.3, 766.5, 1059.7, 1125.0, 1243.1 keV levels have been tentatively identified. The tentative assignment is only because the experimental information was not enough to conclusively determine whether the 758.3 and 760.7 keV transitions decay to ground state or the first excited state at 5.7 keV. Therefore, all these states, except the 758.3 keV, would lie 5.7 keV lower than their present values. On the other hand, if the 758.3 keV transition decays to the first excited state, then there would be a level at 764.0 instead of 758.3 keV.

The 623.5 keV level is a puzzle, as it does not decay to any of the established levels. This could be understood as being due to small branching intensities from this state to low-lying states, which could be below the detection limit of the experimental setup. The evidence for this level is as follows. The strongest 591.8 keV transition has 537.0 and 491.8 keV transitions in coincidence. Further, the 491.8 keV transition has 492.7 and 436.2 keV γ rays in coincidence. But the 436.2 keV transition is not in coincidence with the 537.0 keV transition. Therefore, the 436.2 and 492.7 keV transitions decay in parallel with the 537.0 keV transition, but are in coincidence with each other. There is a weak 392.2 keV transition in coincidence with the 537.0 keV γ ray, and sum up to 929.2 keV, equaling the sum of 436.2 and 492.7 keV. This analysis, therefore, requires a level at 199.9 [591.8 + 537.0 − (492.7 + 436.2)] keV above the

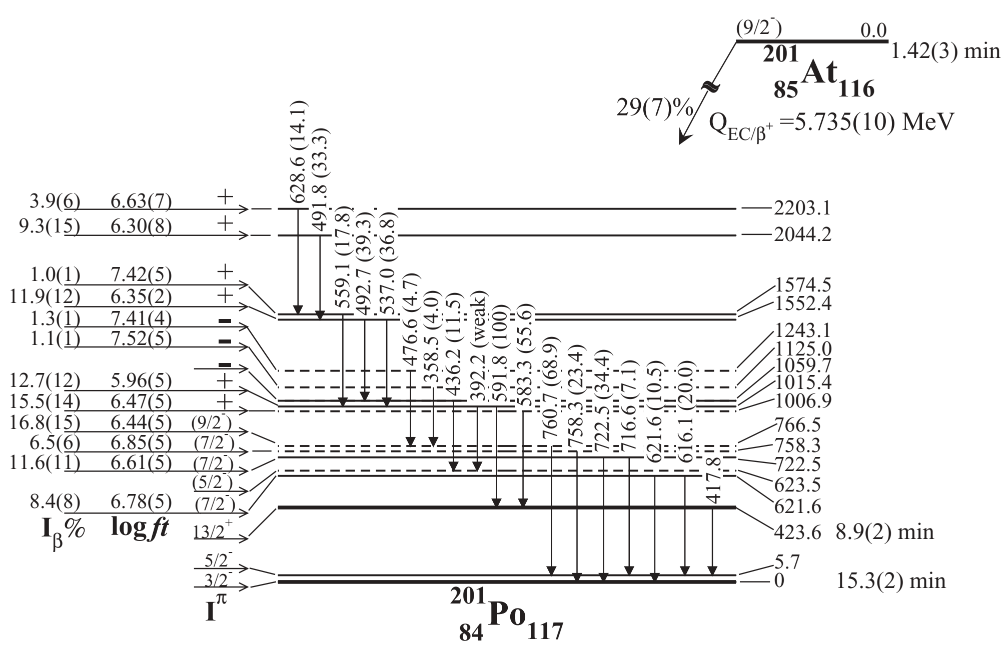

FIG. 7. Level scheme of ^{201}Po as obtained from the β decay of ^{201}At. All the transitions are labeled with their energies and relative γ-ray intensities in brackets. The numbers on the right indicate the excitation energy of each level. Only the parity assignment is shown when it was not possible to determine a level spin. All the half-lives and EC/β^+ branching ratio are from Ref. [15], while the Q value is from Ref. [14].

level where the strongest 591.8 keV level decays. Therefore, if the 591.8 keV transition is placed above the ground state or the first excited state, then a level at 199.9 or 205.6 keV, respectively, is required, which is not possible to explain (see Sec. IV B). Hence we place it above the isomeric $\frac{13}{2}^+$ level at 423.6 keV. This gives rise to a level at 623.5 (=423.6 + 199.9) keV. Further, the conversion coefficient measurements require the assignment of negative parity to this level. The only parity changing transition (492.7 keV) has $E1$ multipolarity.

All the other levels are established on the basis of coincidence relationships and conversion coefficient measurements. The multipolarities of the transitions were determined from the comparison of measured K-shell conversion coefficients with the theoretical values for various multipolarities as shown in the Table II.

IV. DISCUSSION

A. ^{205}Rn

There are two different values for an upper limit to the EC/β^+ branching of ^{205}Fr from earlier studies. Hornshøj *et al.* [1] have set the upper limit to be 3%; while according to the study by Ritchie *et al.* [18], the upper limit is 1%. Only the limits were determined due to nonobservation of γ-ray transitions in ^{205}Rn following EC/β^+ decay of ^{205}Fr. In our work, we determine this branching to be 1.5(2)% from the intensities of the γ-ray transitions in ^{201}Po and ^{205}Rn.

The ground-state spin-parity $I^\pi = \frac{5}{2}^-$ of ^{205}Rn was known from hyperfine structure and isotope shift investigations [11]. A study by Novak *et al.* [12] using a heavy-ion fusion-evaporation reaction has established positive-parity high-spin states in ^{205}Rn above the $\frac{13}{2}^+$ isomeric state. However, no excited negative-parity states were known, but these are expected to occur as the result of the coupling of the odd neutron with the positive-parity core states. The shell-model orbitals accessible to the odd neutron at low energies are $f_{5/2}$, $p_{3/2}$ and $p_{1/2}$ for negative parity and $i_{13/2}$ for positive parity. The levels at 0, 31.4, and 657.1 keV could be understood as one-quasiparticle states originating from coupling the odd $f_{5/2}$, $p_{3/2}$ and $i_{13/2}$ neutron to the 0^+ ground state of the core, respectively. However, it was not possible to establish the $\frac{1}{2}^-$ state. This is also not unexpected, since only the states with spin values near to the parent ground-state spin of $I^\pi = \frac{9}{2}^-$ would be strongly populated in the β decay, due to selection rules.

A better understanding of the observed states could be obtained by the systematic comparison of Pb, Po, and Rn isotones with $N = 123$, 121, and 119, which have the same ground-state spin-parity. In the case of $\frac{3}{2}^-$, the excitation energy decreases with decreasing neutron number and increasing proton number from 263 keV for ^{205}Pb ($Z = 82$, $N = 123$) to 62 keV for ^{203}Po ($Z = 84$, $N = 119$). If the same trend prevails for ^{205}Rn ($Z = 86$, $N = 119$), then the $\frac{3}{2}^-$ level should have an excitation energy less than 62 keV. The $\frac{3}{2}^-$ level observed at 31.4 keV in the present work fits very well with this trend, as shown in Fig. 8(a). A similar analysis can be done for the $\frac{13}{2}^+$ levels. The energy of this level is observed to decrease with decreasing neutron number, e.g., from 1014 keV ($Z = 82$, $N = 123$) to 629 keV ($Z = 82$, $N = 119$) and increases with increasing proton number, e.g., to 1173 keV ($Z = 86$, $N = 123$). The tentative level at 657.1 keV in ^{205}Rn ($Z = 86$, $N = 119$) also fits well the

TABLE II. γ-ray energies, relative intensities along with the experimental and theoretical [13] K-shell conversion coefficient and assigned multipolarity for transitions in ^{201}Po. The energies are accurate to within 0.2 keV for $I_\gamma \geqslant 10$ and 0.4 keV for $I_\gamma < 10$.

Transition energy (keV)	Relative intensity (I_γ)	Experimental K-conversion coefficient (10^{-2})	Theoretical K-conversion coefficient			Assigned multipolarity
			$E1$ (10^{-2})	$E2$ (10^{-2})	$M1$ (10^{-2})	
358.5	4.0(4)					
392.2	weak					
417.8[a]						
436.2	11.5(10)	9.4(14)	1.12	2.95	14.95	$M1+E2$
476.6	4.7(5)					
491.8	33.3(51)	2.3(7)	0.87	2.29	10.86	$E2$
492.7	39.3(60)	1.0(4)	0.87	2.28	10.81	$E1$
537.0	36.8(31)	2.4(3)	0.73	1.92	8.60	$E2+M1$
559.1	17.8(16)	3.2(5)	0.67	1.77	7.73	$E2+M1$
583.3	55.6(46)	2.3(3)	0.62	1.62	6.92	$E2+M1$
591.8	100	2.2(3)	0.60	1.58	6.66	$E2+M1$
616.1	18.6(16)	2.6(4)	0.56	1.46	5.99	$E2+M1$
621.6	10.5(9)	1.9(3)	0.55	1.43	5.85	$(E2+M1)$
628.6	14.1(20)	1.4(3)	0.53	1.40	5.68	$E2$
716.6	7.1(6)					
722.5	34.4(29)	0.8(1)	0.41	1.07	3.95	$E2$
758.3	23.4(20)	0.7(1)	0.37	0.97	3.48	$E2$
760.7	68.9(57)	0.9(1)	0.37	0.97	3.46	$E2$

[a]Unobserved in the present work due to longer isomer half-life than the measurement time. Energy from Ref. [15].

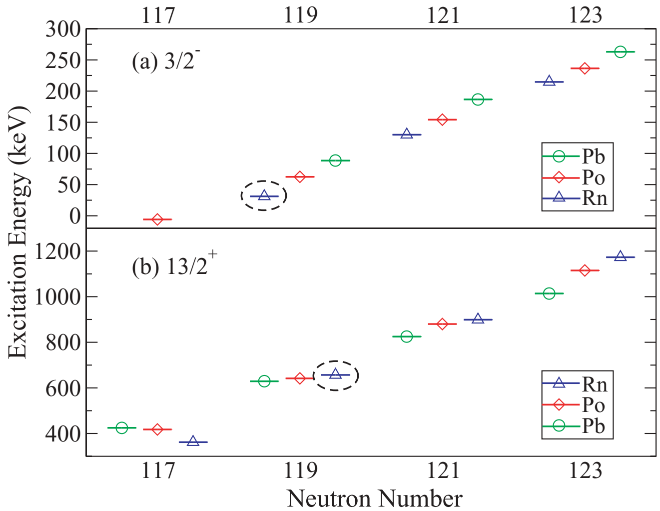

FIG. 8. (Color online) Systematics of excitation energy of (a) $\frac{3}{2}^-$ and (b) $\frac{13}{2}^+$ levels with respect to $\frac{5}{2}^-$ in Pb, Po, and Rn, for neutron numbers 117, 119, 121, and 123. The dashed ellipses show the new findings from the present work.

increasing trend (629.1-641.7-657.1 keV) of $\frac{13}{2}^+$ level energy along the $N = 119$ isotones in Pb-Po-Rn nuclei as depicted in Fig. 8(b). There is a noticeable discrepancy in the level scheme of ^{205}Rn presented by Novak *et al.* in Ref. [12]. It is known that the 633.1 keV transition in ^{205}Rn decays to the ground state [4]. The energy difference between the ground state and the isomeric $\frac{13}{2}^+$ level as calculated from the level scheme presented in Ref. [12] is found to be 93 [$= 634 + 673 + 466 - (500 + 1180)$] keV. However, this difference is expected to be around 650 keV from the systematics [see Fig. 8(b)]. Therefore, we conclude that some transitions are missing in the sequence 634-673-466 keV in Ref. [12]. This conclusion can also be reached from other arguments. The ground-state spin-parity of ^{205}Rn is known to be $\frac{5}{2}^-$ from Ref. [11]. If we assume maximum $\Delta J = 2$ for each transition in the 634-673-466 keV sequence, then we will get $J = \frac{17}{2}$ for the level that is depopulated by the 466 keV transition, while it is established to be $\frac{21}{2}^+$ [12]. This implies that one transition with spin $2\hbar$ or two each with spin $1\hbar$ are missing between the ground state and the $\frac{21}{2}^+$ state in Ref. [12].

The states around 600 keV could be understood as states originating from the coupling of the odd neutron in $f_{5/2}$, $p_{3/2}$, and $p_{1/2}$ orbitals to the 2^+ even-even core state (e.g., at 575.3 keV in ^{206}Rn). Such a coupling actually results in one $\frac{9}{2}^-$ state, two $\frac{7}{2}^-$ states, three each of $\frac{5}{2}^-$, $\frac{3}{2}^-$, and two $\frac{1}{2}^-$ levels. However, not all of them could be observed in the present work, since they are not very strongly populated in the β decay of the $\frac{9}{2}^-$ ground state of ^{205}Fr. Similar considerations suggest that a large number of states should also be found near 1100 keV (from coupling to the 4^+ core state), 1700 keV (from coupling to the 6^+ and 8^+ core states), and so on. The two groups around 600 and 1050 keV fit the expected pattern quite well, as is evident from Fig. 4.

B. ^{201}Po

In the case of ^{201}Po, four one-quasiparticle states at 0.0, 6.3, 142, and 424.1 keV corresponding to coupling of $p_{3/2}$, $f_{5/2}$, $p_{1/2}$, and $i_{13/2}$ shell-model orbitals to the 0^+ ground state of neighboring cores, respectively, were known prior to this study [15]. All the above levels, except the $\frac{1}{2}^-$, have been identified in the present work. The $\frac{5}{2}^-$ and $\frac{13}{2}^+$ levels have been established at 0.6 keV lower in energy than their previous values.

On the basis of similar arguments to those for ^{205}Rn, negative-parity states around 700 keV can be understood as being due to the coupling of the above shell-model orbitals to the 2^+ state of an even-even core. Also, such a coupling with the 4^+ core state gives rise to several states around 1250 keV. This is reflected in Fig. 7, where two groups of negative-parity states around 700 and 1100 keV are evident.

The positive-parity states can be obtained by coupling the $i_{13/2}$ neutron to neighboring even-even core states. Thus, at about 700 keV above the isomeric state, there should be one state each with spin-parity $\frac{9}{2}^+$, $\frac{11}{2}^+$, $\frac{13}{2}^+$, $\frac{15}{2}^+$, and $\frac{17}{2}^+$ due to coupling with the 2^+ state. Similarly, more states with a wider spin range should be observed near 1650 and 2100 keV due to such a coupling with 4^+ and 6^+, respectively. However, according to the β-decay selection rules, only $\frac{9}{2}^+$ and $\frac{11}{2}^+$ are expected to be populated strongly. The groups of two positive-parity states are clearly visible around 1000, 1550, and 2100 keV. It is not clear to us why the positive-parity states are populated more strongly than the negative-parity states when the ground state of the parent nucleus has negative parity. The $\log ft$ values of all the levels (see Fig. 7) are in accordance with the β-decay selection rules.

V. SUMMARY

Excited states in ^{205}Rn and ^{201}Po populated in EC/β^+ decay were studied using γ-ray and conversion-electron spectroscopy at ISOLDE, CERN. Several new γ-ray transitions were identified for the first time. The EC/β^+ branch from ^{205}Fr was determined to be 1.5(2)%. The new transitions establish 5 and around 14 hitherto unknown levels in ^{205}Rn and ^{201}Po, respectively. The $\log ft$ values for the newly established levels have also been deduced from intensity balances. The newly identified $\frac{3}{2}^-$ level at 31.4 keV and tentative $\frac{13}{2}^+$ level at 657.1 keV in ^{205}Rn fit very well into the systematics of neighboring even-odd isotopes and are identified as neutron $p_{3/2}$ and $i_{13/2}$ shell-model orbitals, respectively. Also, the neutron $f_{5/2}$ shell-model orbital in ^{201}Po has been fixed at 5.7 keV. All the negative-parity levels in both these nuclei are explained as being due to the coupling of the odd neutron in $f_{5/2}$, $p_{3/2}$, and $p_{1/2}$ orbitals with the neighboring even-even core states, while the positive-parity levels are part of the same coupling but due to the unique positive-parity $i_{13/2}$ shell-model orbital available near the Fermi surface. Further work to unambiguously determine the excitation energy and the half-life of the one-quasiparticle $i_{13/2}$ isomer in ^{205}Rn would be valuable.

ACKNOWLEDGMENTS

The authors thank the ISOLDE technical staff for their assistance during the experiment. Financial support from the UK STFC and AWE plc, the Spanish MEC FPA2007-07393, CSPD-2007-00042 CPAN, FPA2005-03993, and FPA 2008-06419-C02-01 projects is gratefully acknowledged. A.A. also acknowledges partial support from the Ramon y Cajal program.

[1] P. Hornshøj, P. G. Hansen, and B. Jonson, Nucl. Phys. **A230**, 380 (1974).
[2] B. Jonson, M. Alpsten, A. Appelqvist, and G. Astner, Nucl. Phys. **A174**, 225 (1971).
[3] J. Wauters, P. Dendooven, M. Huyse, G. Reusen, P. Van Duppen, and P. Lievens, Phys. Rev. C **47**, 1447 (1993).
[4] F. P. Heßberger, S. Hofmann, and D. Ackermann, Eur. Phys. J. A **16**, 365 (2003).
[5] U. Köster (ISOLDE Collaboration), Radiochim. Acta **89**, 749 (2001).
[6] J. van Klinken and K. Wisshak, Nucl. Instrum. Methods **98**, 1 (1972).
[7] J. van Klinken and K. Wisshak, Nucl. Instrum. Methods **130**, 427 (1975).
[8] http://www.xia.com/DGF_Pixie-4.html.
[9] D. C. Radford, Nucl. Instrum. Methods Phys. Res. A **361**, 297 (1995).
[10] F. G. Kondev, Nucl. Data Sheets **101**, 521 (2004), and references therein.
[11] W. Borchers *et al.*, Hyperfine Interact. **34**, 25 (1987).
[12] J. R. Novak *et al.*, Phys. Rev. C **59**, R2989 (1999).
[13] T. Kibédi, T. W. Burrows, M. B. Trzhaskovskaya, P. M. Davidson, and C. W. Nestor Jr., Nucl. Instrum. Methods A **589**, 202 (2008).
[14] G. Audi, A. H. Wapstra, and C. Thibault, Nucl. Phys. **A729**, 337 (2003).
[15] F. G. Kondev, Nucl. Data Sheets **108**, 365 (2007), and references therein.
[16] S. Axensten, G. Liljegren, I. Lindgren, and C. M. Olsmats, Ark. Fys. **22**, 392 (1962).
[17] T. Weckström, B. Fant, T. Lönnroth, V. Rahkonen, A. Källberg, and C.-J. Herrlander, Z. Phys. A **321**, 231 (1985).
[18] B. G. Ritchie, K. S. Toth, H. K. Carter, R. L. Mlekodaj, and E. H. Spejewski, Phys. Rev. C **23**, 2342 (1981).